Stem Cell Reports
Review
ISSCR
OPEN ACCESS

Stem cell-based vascularization of microphysiological systems

Shane Browne,[1,3] Elisabeth L. Gill,[1,3] Paula Schultheiss,[1] Ishan Goswami,[1,2] and Kevin E. Healy[1,2,*]
[1]Department of Bioengineering and California Institute for Quantitative Biosciences (QB3), University of California at Berkeley, Berkeley, CA 94720, USA
[2]Department of Materials Science and Engineering, University of California, Berkeley, CA 94720, USA
[3]These authors contributed equally
*Correspondence: kehealy@berkeley.edu
https://doi.org/10.1016/j.stemcr.2021.03.015

SUMMARY

Microphysiological systems (MPSs) (i.e., tissue or organ chips) exploit microfluidics and 3D cell culture to mimic tissue and organ-level physiology. The advent of human induced pluripotent stem cell (hiPSC) technology has accelerated the use of MPSs to study human disease in a range of organ systems. However, in the reduction of system complexity, the intricacies of vasculature are an often-overlooked aspect of MPS design. The growing library of pluripotent stem cell-derived endothelial cell and perivascular cell protocols have great potential to improve the physiological relevance of vasculature within MPS, specifically for *in vitro* disease modeling. Three strategic categories of vascular MPS are outlined: self-assembled, interface focused, and 3D biofabricated. This review discusses key features and development of the native vasculature, linking that to how hiPSC-derived vascular cells have been generated, the state of the art in vascular MPSs, and opportunities arising from interdisciplinary thinking.

INTRODUCTION

Microphysiological systems (MPSs), also termed organ or tissue chips, use microfluidics and 3D cell culture to mimic tissue and organ-level physiology. While MPSs have classically been fabricated using soft lithography, more recently other methods have evolved that offer competitive advantages for certain applications, most prominently 3D printing. MPSs have been used to organize and observe co-cultures in 3D (Kurokawa et al., 2017; Lin et al., 2019), cell-biomaterial interactions (Natividad-Diaz et al., 2019), and tissue properties such as permeability (Qiu et al., 2018; Stebbins et al., 2019). They may be designed to generate chemotactic gradients, fluidic shear stress, or localized mechanical and electrical stimulation (Pavesi et al., 2015), or to facilitate molecular or cellular diffusion (Zhang et al., 2016a) in addition to incorporating non-invasive sensory capabilities (Park et al., 2019; Stebbins et al., 2019; Yeste et al., 2017). The advent of human induced pluripotent stem cell (hiPSC) technology has accelerated MPSs' usefulness in the study of human disease and drug testing in a range of organ systems (Mathur et al., 2013).

To reduce system complexity, the vasculature is an often-overlooked aspect of MPS design. For instance, many MPSs model vascular perfusion through use of microfluidic geometry such as micropillars, semi-permeable 2D membranes, or as a simple endothelial cell (EC) monolayer. Vasculature is a responsive network that acts as a semi-permeable barrier controlling two-way transport of a wide range of small and macromolecules, including gases (i.e., O_2, CO_2), saccharides, fatty acids, and proteins. In addition to its critical function in tissue perfusion, signaling between vascular and non-vascular cells in the microenvironment, termed angiocrine signaling, provides biological cues that actively support tissue homeostasis, metabolism, and regeneration (Ramasamy et al., 2015). Vasculature also plays an integral role in many pathologic conditions, such as vascular malformations, cardiovascular disease, cancer, inflammation, and diabetes (Muller, 2013; Qiu et al., 2018; Sewell-Loftin et al., 2020). In the case of cancer, the formation of new blood vessels in the tumor microenvironment is a key driving factor in the progression of the disease and has been identified as a potential therapeutic target.

This review looks to the organization of vasculature in native tissues in terms of the constituent cell types and their roles in vascular development and homeostasis. The directed differentiation of ECs, pericytes (PCs), smooth muscle cells (SMCs), and fibroblasts (FBs) from hiPSCs is discussed, with a view to recapitulating human vasculature within MPS. Next, a summary of the state of the art in perfusable vasculature within MPSs is presented with evaluation of their strategic strengths and the advances made using hiPSCs. Finally, key approaches are identified to enhance the physiological relevance of vascularized MPS, realize the construction of human isogenic MPSs, and drive their acceleration toward clinical accuracy.

Blood vessel development

Blood vessels are composed of three layers: the intima, media, and adventitia. The inner (intima) layer is composed of ECs, while the middle (media) layer comprises perivascular cells (PVCs), predominantly SMCs and PCs. The external adventitia is a collagen-rich connective tissue containing stromal cells (SCs), principally FBs. Blood vessel development begins with the *de novo* assembly of a primitive vascular network by ECs, although these nascent vessels are inherently unstable and will regress without adequate support (Jain, 2003). Platelet-derived growth factor (PDGF) BB, secreted by ECs in response to shear stress, promotes the recruitment of PVCs to support nascent vessels (Resnick et al.). Evidence suggests that EC-PC interaction

via TGF-β1 also plays a role in vessel maturity and stabilization (Walshe et al., 2009). Interestingly, TGF-β1 has also been implicated in EC development (Perlingeiro, 2007) and the initial stages of vascularization, including proliferation, migration, and tube formation, through the endoglin (CD105) co-receptor (Browne et al., 2018; Lebrin et al., 2004). For an in-depth description of vascular development, including venous versus arterial specification, we refer the reader to a recent review from Niklason and Dai (2018).

Vascular cell types

ECs

ECs are the central component of the vascular system, providing a non-thrombotic surface lining the lumen of vessels. ECs emerge from a common precursor, the angioblast, derived from the mesoderm during development. Once the main vascular plexus is established, new vascular beds develop to supply organs depending on their metabolic need through a combination of vasculogenesis and sprouting angiogenesis, the growth of new blood vessels from pre-existing vessels (Chung and Ferrara, 2011).

ECs demonstrate great variability in their function and phenotype, and may be categorized by their arterial or venous phenotype, or their tissue specificity (e.g., heart, brain, liver, lung) (Augustin and Koh, 2017). EC subtypes differ significantly with regard to properties such as expression of surface markers, transporter molecules, and secretion of paracrine signals. The most commonly described cell surface marker of the arterial endothelium is Ephrin B2 (EphB2), required for vasodilation in response to fluid flow or acetylcholine (Lin et al., 2014). Additionally, arterial ECs express higher levels of Notch ligands and receptors compared with venous ECs as well as several gap junction proteins, including Cx37, Cx40, and Cx46 (Cui et al., 2015). In contrast, the venous endothelium is marked by the expression of EphB4 and COUP-TFII, the latter of which may play a role in the increased resistance of veins to vascular disease (Cui et al., 2015).

A unique feature of the arterial system is the regulation of vascular tone, controlling blood flow by altering vessel diameter (Sandoo et al., 2010). To this end, ECs are excellent mechanosensors: arterial ECs respond to changes in wall shear stress through release of vasodilating and constricting factors such as nitric oxide (NO) or endothelin to communicate with SMCs and adjust vessel tone (Chatterjee and Fisher, 2014). Typical wall shear stress in the arterial system ranges from 10–40 dynes/cm^2, while wall shear stress in veins is significantly lower at 1–5 dynes/cm^2 (Malek, 1999). Lower wall shear stress in the venous system provides a suitable environment for leukocyte adhesion. The expression of leukocyte adhesion molecules such as E- and P-selectin and the lack of highly organized tight junctions in post-capillary venules facilitates the invasion of immune cells to sites of inflammation (Muller, 2013).

Exchange of nutrients and waste primarily occurs in capillary networks, where organ-specific capillary ECs regulate permeability and transporter function to meet the metabolic needs of a tissue (Augustin and Koh, 2017). As an example, the endothelium of the blood-brain-barrier (BBB) is unique in its highly selective barrier function, due to high expression of organized tight junctions and adherens junctions reducing paracellular transport across the endothelium (Zhao et al., 2015). Conversely, microvascular ECs of organs responsible for absorption and filtration, such as kidney or liver, allow rapid exchange between blood and tissue (Satchell and Braet, 2009). Tissue-specific microvasculature can also adjust to the metabolic demands of the underlying tissue by expressing selective transporter molecules: myocardial ECs facilitate the uptake of fatty acids, the preferred adenosine triphosphate (ATP) source for cardiomyocytes, via the fatty acid transporter CD36 (Coppiello et al., 2015).

The endothelium not only acts as a highly specific barrier between tissue and blood but ECs also secrete a variety of paracrine and matrix signals, resulting in dynamic crosstalk with the surrounding parenchymal cells and play an active role in the development, regeneration, and metabolism of the specific tissue. Examples include the secretion of hepatocyte growth factor (HGF) by liver sinusoidal ECs (LSECs), which aids in liver regeneration (Yamane et al., 1994), or deposition of laminin-alpha 4 and 5 chains by pancreatic ECs stimulating insulin production by islet cells (Nikolova et al., 2006).

Tissue specificity is an important consideration regarding ECs, as this has been demonstrated to play a critical role not only in regulation of molecular transport as alluded to above but also in other contexts. For example, with regard to viral tropism, it has been shown that islet ECs upregulate the expression of decay accelerating factor (DAF), human coxsackievirus and adenovirus receptor (HCAR), and integrin $\alpha_V\beta_3$ in response to coxsackievirus infection (Zanone et al., 2007). Contrasting behaviors have been observed with DAF and HCAR expression in human umbilical vein ECs (HUVECs), aortic ECs, and dermal ECs, highlighting the dependence of infection on tissue-specific ECs. Ware et al. (2018) demonstrated that co-culture of primary human hepatocytes with primary LSECs improved albumin secretion of the hepatocytes over an 11-day period compared with hepatocytes alone. This effect was not observed with HUVECs or immortalized LSECs, demonstrating the importance of tissue specificity and the inability of immortalized LSECs to accurately represent the appropriate phenotype.

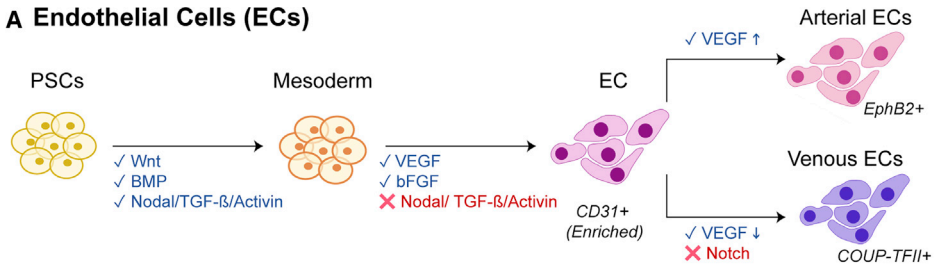

(Harding et al., 2017; Orlova et al., 2014; Rosa et al., 2019; Zhang et al., 2017)

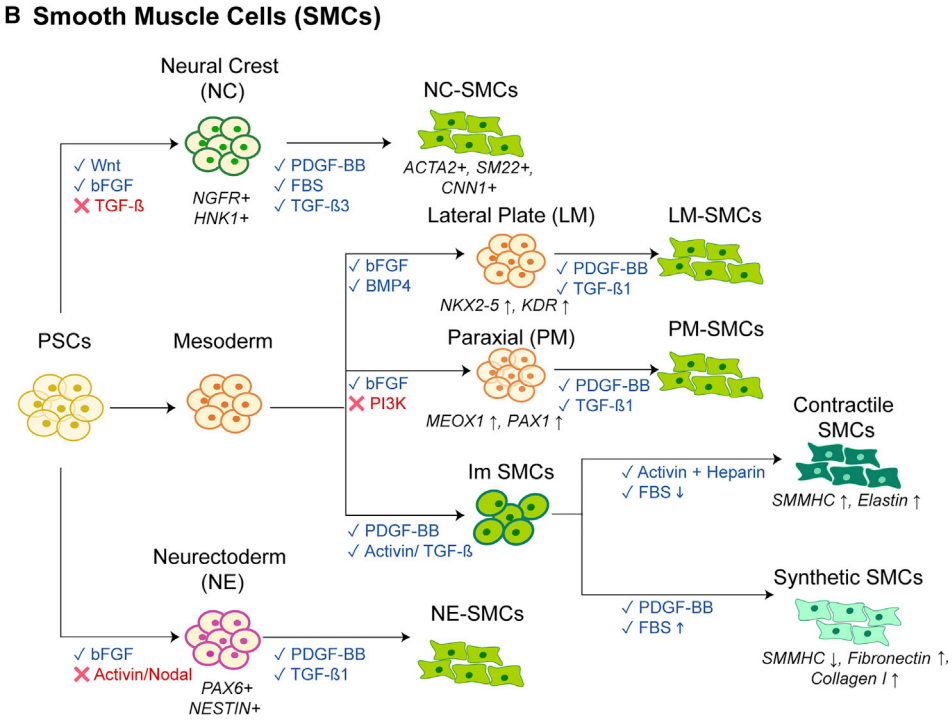

(Cheung et al., 2012; Kumar et al., 2017; Patsch et al., 2015; Wanjare et al., 2014)

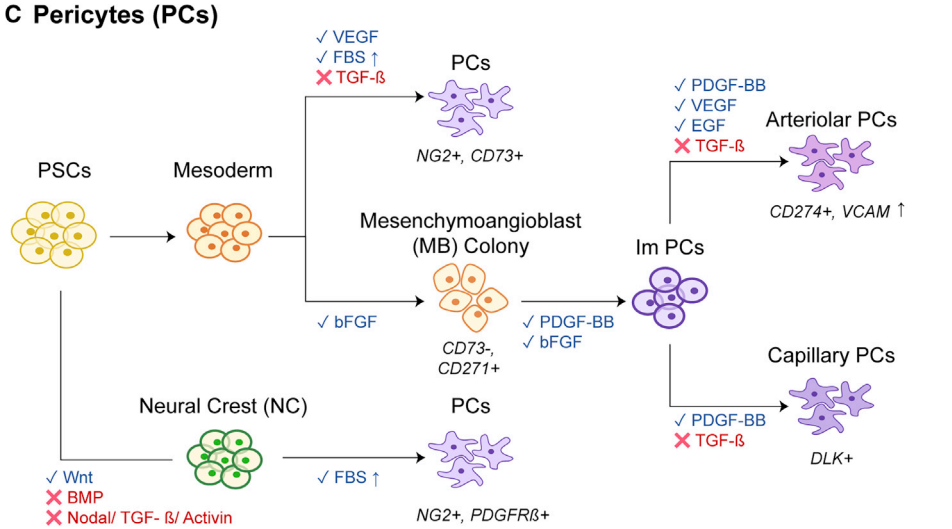

(Kumar et al., 2017; Orlova et al., 2014; Stebbins et al., 2019)

(legend on next page)

Perivascular and SCs

PVCs wrap around vessels, providing trophic support and extracellular matrix (ECM) to ensure maturation and stabilization of the neovasculature (Gaengel et al., 2009). The interaction between angiopoietins (Ang-1 and Ang-2) and Tie-2 receptor plays a critical role in vessel homeostasis and angiogenesis, including vascular remodeling and the shift from endothelial quiescence to activation (Isidori et al., 2016; Thomas and Augustin, 2009). PVCs produce Ang-1, which promotes vascular homeostasis, basement membrane deposition, EC quiescence, and tight barrier function. In contrast, Ang-2 is secreted by ECs during hypoxia and tissue injury, promoting vascular instability. This can lead to vascular regression, or to branching angiogenesis in the presence of angiogenic growth factors such as vascular endothelial growth factor (VEGF).

SMCs are prevalent surrounding larger vessels, providing contractility and reinforcing barrier function as they wrap perpendicularly around the long axis of vessels (Wanjare et al., 2013). They may be subdivided into contractile and synthetic SMCs. Contractile SMCs are quiescent and characteristic of healthy adult vessels, with an elongated and spindle-shaped morphology. Conversely, synthetic SMCs are smaller and have a less elongated morphology (Wanjare et al., 2013, 2014). Synthetic SMCs predominate in embryonic growth and injured or diseased tissue, and thus are substantially more migratory and proliferative (Wanjare et al., 2014).

PCs perform similar functions to SMCs but are typically found surrounding smaller blood vessels and capillaries (Wanjare et al., 2013). However, this distinction is not definitive as intermediate phenotypes between SMCs and PCs have been described on mid-sized vessels. This is not surprising given that SMCs and PCs are thought to be derived from the same lineage. In general, pericytes display an elongated, stellate morphology *in vivo*; however, their distribution and orientation vary by location: they align parallel to capillaries but wrap around microvessels circumferentially. Similar to ECs, both PCs and SMCs display tissue-specific characteristics. For instance, BBB pericytes play a key role in reducing nonspecific molecular transcytosis and possess brain-specific molecular markers identifiable through transcript analysis and RNA sequencing (Stebbins et al., 2019).

In addition to the direct interaction between ECs and PVCs, FBs can direct the characteristics and growth of blood vessels (Newman et al., 2011). While primarily recognized for their role in ECM deposition and remodeling, FBs also provide paracrine support for angiogenesis, particularly during tissue injury and regeneration (Newman et al., 2013). A range of studies have interrogated the support FBs provide to ECs during vascular network formation, and evidence exists that they play a role in paracrine support (Martin et al., 1999), ECM remodeling, and deposition (Romero-López et al., 2017).

Differentiation of vascular cells from pluripotent cells

ECs

ECs derived from pluripotent stem cells (PSCs) or induced-PSCs (iPSCs) offer a potentially limitless supply of vascular cells and provide a single genetic background for the co-culture of multiple cell types, as well as the capacity to study specific disease populations (Liu et al., 2018). Early EC differentiation protocols relied on embryoid bodies, typically requiring several weeks, resulting in a heterogeneous mix of cells from all three germ layers with a relatively low yield of ECs (<5%). More recently, 2D directed differentiation protocols have come to the fore. These approaches mostly follow a similar trajectory; an initial step focusing on mesoderm induction, and thereafter the specialization of the mesoderm progenitors toward the vascular lineage (Figure 1A).

Several pathways stimulate mesoderm induction, including signaling pathways such as Nodal, fibroblast growth factors (FGFs), BMPs, and Wnts (Gadue et al., 2006). The Wnt signaling pathway can be promoted by addition of GSK-3 (glycogen synthase kinase 3) inhibitors such as CHIR99021 or BIO (6-bromoindirubin-3′-oxime) (Harding et al., 2017; Orlova et al., 2014; Zhang et al., 2017). A commonly used activator for the Nodal signaling pathway is Activin A, which induces nuclear translocation of transcription factors essential for mesoderm formation such as Smad2/3 (Naujok et al., 2014). Likewise, the addition of BMP4, another member of the TGF-beta superfamily, activates similar pathways and induces mesoderm formation (Orlova Valeria et al., 2014).

The MAPK pathway is responsible for the expression of the early mesoderm transcript, Brachyury, and can be induced by addition of basic FGF (bFGF) (Harding et al., 2017). While TGF-β/Nodal/Activin signaling is vital for mesoderm induction (Gadue et al., 2006), the timely withdrawal of early mesoderm induction factors such as BMP-4 has been shown to improve EC specification. Accordingly, the inhibition of canonical TGF-β signaling via the small molecule SB-431542 post-mesoderm induction enhances EC specification (Harding et al., 2017).

Figure 1. Differentiation of ECs, SMCs, and pericytes

Schematic diagrams of (A) EC, (B) smooth muscle cell, and (C) pericyte differentiations. Supplemental factors and upregulated pathways appear in blue with a tick, inhibited pathways with a red cross, and black italicized text denotes a characteristic cell or ECM markers or gene expression. Positive expression is indicated by +; upregulation and downregulation of a marker or factor by ↑ and ↓ respectively.

Mesoderm progenitors have the potential to differentiate into a range of cell types; thus, signals must be provided to drive endothelial specification. The most potent and well-known inducer of endothelial specification is VEGF. As a key regulator of vasculogenesis and angiogenesis, VEGF supplementation drives MAPK, ROCK/Rho, and Notch signaling pathways (Wang et al., 2013). VEGF supplementation is an essential step in many protocols for EC differentiation (Kusuma et al., 2013), sometimes in combination with other pro-angiogenic molecules such as bFGF or thymosin beta 4 (Tβ4) (Rosa et al., 2019). Other biochemical cues, such as hypoxia, have been shown to enhance VEGF signaling and more closely recapitulate the environment of the developing embryo (Prado-Lopez et al., 2009).

These approaches generate a heterogeneous mixture of cells, of which ECs typically constitute 30%–40% of the population (Kurokawa et al., 2017; Kusuma et al., 2013; Natividad-Diaz et al., 2019). Thus, differentiation protocols often involve purification of ECs from the non-ECs population. Magnetic activated cell sorting (MACS) or fluorescence-activated cell sorting (FACS), selecting for markers such as CD31, VE-cad, and KDR/VEGFR2 isolate a high-purity EC population, exhibiting classic cobblestone morphology in 2D culture. Confirmation of EC phenotype requires analysis of phenotypic markers via flow cytometry or immunostaining. Functional assays include the Matrigel tube formation assay, uptake of acetylated low-density lipoprotein (Ac-LDL) and measurement of NO production. EC barrier function can be measured via transwell permeability studies or measurement of transendothelial electrical resistance (TEER). Recently, a consensus has been published describing key assays to study angiogenesis, many of which are relevant to studying the angiogenic potential of differentiated ECs *in vitro*, *ex vivo*, and *in vivo* (Nowak-Sliwinska et al., 2018). These include *in vitro* assessment of ECs migration, proliferation, 3D vascular morphogenesis, and the interaction with PVCs, all of which are relevant for MPS.

Perivascular and SCs

In addition to ECs, the derivation of PVCs and SCs is a critical consideration for a more physiologically relevant MPS. A significant proportion of the existing literature uses 2D directed differentiation approaches to generate PVCs and SCs, as opposed to embryoid body or feeder layer strategies. Protocols for chemically directed 2D differentiation of SMCs and PCs typically direct cells down a mesoderm or neural crest lineage (Cheung et al., 2012). The vasculature of certain tissues has been associated with specific lineages, which guides their differentiation strategy. One recent study generated PCs from a neural crest lineage to mimic the developmental origins of central nervous system mural cells in a BBB model (Stebbins et al., 2019). SMCs and PCs have considerable phenotypic overlap, sharing embryonic origin, complicating the distinction between both cell types (Cheung et al., 2012; Wanjare et al., 2014). Existing protocols for generating SMCs, PCs, and FBs from PSCs have a varied approach, and several of the most widely used methods are summarized graphically in Figures 1B and 1C.

SMCs can be generated from several intermediate embryonic lineages; differences between these subtypes have been used to study regional tissue susceptibility to developmental diseases, such as Marfan syndrome (Cheung et al., 2012; Granata et al., 2017). During the intermediate specification stages, cells are supplemented with PDGF-BB, simulating EC signaling, and a high serum concentration. Distinct maturation stages for contractile and synthetic SMCs have also been outlined (Patsch et al., 2015; Wanjare et al., 2013). Maturation of a contractile phenotype can be achieved with deprivation of PDGF-BB and serum, whereas continuous supplementation leads to a synthetic phenotype (Patsch et al., 2015; Wanjare et al., 2014). An alternative protocol that used a mesenchymoangioblast precursor similarly used a MEK inhibitor to halt cell proliferation and induce a more mature phenotype (Kumar et al., 2017). In addition to PDGF-BB, TGF-β1 is another prevalent induction factor, with sustained supplementation during SMC maturation (Cheung et al., 2012). Broadly reported markers expressed by SMCs include αSMA and SM22 (Wanjare et al., 2013). The contractile phenotype expresses heavy chain caldesmon, calponin, smoothelin, and notably smooth muscle myosin heavy chain (SMMHC) in the late stages of maturation, whereas synthetic SMCs can be distinguished by light chain caldesmon and vimentin expression (Wanjare et al., 2013). The key functionality assessed to distinguish contractile SMCs from PCs is cell contractility, measured via changes in cell area following stimulation with carbachol or other vasoactive drugs such as endothelin and atropine (Patsch et al., 2015). Calcium imaging can provide additional quantified measurement of contractility (Halaidych et al., 2019; Patsch et al., 2015). In addition, the ECM deposited by contractile SMCs was shown to contain elastin and a higher collagen I content compared with synthetic SMCs and PCs (Wanjare et al., 2014).

PC differentiation typically involves similar signaling pathways to endothelial differentiation. Commonly protocols feature a mesoderm induction step using some combination of FGFs, BMP4, Activin A, and WNT inhibition, followed by ALK-4/5/7 signaling inhibition via SB431542 and PCs specification with growth factors such as VEGF, PDGF-BB, and bFGF (Kumar et al., 2017; Orlova et al., 2014). As with SMCs, PDGF-BB is the most common factor driving PCs specification. Application of ALK-4/5/7 inhibitor SB431542 has strategically been used to steer differentiation toward a pericyte fate (Kumar et al., 2017; Orlova et al., 2014; Stebbins et al., 2019), inhibiting the transition

to SMCs by suppressing the TGF-β pathway. Additional supplementation with VEGF and epidermal growth factor (EGF) was in one instance used to differentiate between arteriolar and capillary pericytes (Kumar et al., 2017). Functional attributes of PCs used for characterization include the propensity to migrate toward ECs and stabilize tube formation (Kumar et al., 2017; Orlova et al., 2014; Wanjare et al., 2014). A recent study focused on brain PCs and their role in the BBB (Stebbins et al., 2019): hiPSC-derived neural crest PCs and brain microvascular ECs were co-cultured, after which barrier function was assessed through TEER measurement, occludin staining, and transcytosis of dextran (Stebbins et al., 2019). Furthermore, an isogenic neurovascular unit was modeled through integrating the pericyte-like cells with hiPSC-derived brain microvascular ECs, and a mixed population of astrocytes and neurons. The combination of these cell types produced a higher TEER measurement and lower dextran permeability than a monoculture of ECs or co-culture with either one of the other cell groups.

Many protocols for generating FBs are tissue specific and are a byproduct of different cell differentiation processes; e.g., EC or cardiomyocyte. One recent method used data from transcriptome analysis to customize a cardiac FBs differentiation protocol (Zhang et al., 2019). Initially it resembles a cardiomyocyte differentiation, generating epicardial cells, but strategic application of FGF and SB431542 to inhibit ALK-4/5/7 signaling steers cell fate toward a high-purity FBs population. The cells demonstrated stable phenotype after passaging, similar ECM secretion to primary cardiac FBs, and significant promise in modeling cardiac fibrosis and the screening of anti-fibrotic drugs (Zhang et al., 2019). A couple of prominent hiPSC-derived FBs protocols deviate from using 2D directed differentiation (Kim et al., 2018; Shamis et al., 2013). An embryoid body method has been developed to differentiate hiPSC-derived FBs, which were co-cultured with hiPSC-derived keratinocytes to form skin organoids (Kim et al., 2018). Another protocol that used mouse embryonic feeders at the induction stage investigated the ability of embryonic stem cell (ESC) and hiPSC-derived FBs to secrete proangiogenic factors such as VEGF, PDGF-AA, and Ang-1, which stimulated endothelial sprouting (Shamis et al., 2013). *In vitro* co-culture with ECs supported vascular network assembly and basement membrane deposition, indicating the cells acquired a pericyte-like phenotype.

Strategies for the vascularization of microphysiological systems

Recapitulating the vasculature is a critically important step to mimic organ function and develop accurate models of human tissues for disease modeling and drug discovery. Strategies adopted to simulate vasculature within an MPS may be classified broadly into three distinct categories: self-assembly of 3D vascular networks within an ECM, vascular formation on engineered interfaces, and 3D vasculature created via innovative biofabrication techniques. These strategies have relied heavily on primary cells such as HUVECs, but recent advances using PSC/iPSC-derived vascular cells are highlighted.

Self-assembly of 3D vascular networks

A bioinspired approach to generate and integrate vasculature within MPS harnesses the inherent capacity of ECs to self-assemble into a vascular network. This strategy typically involves the assembly and organization of ECs into a 3D vascular structure, with the aim of establishing a perfusable network. Self-assembly approaches have a key benefit: they closely mimic key physiological processes of vascular development, vasculogenesis, and angiogenesis.

The physiological process of EC proliferation and invasion of a suitable ECM to form a vascular network via angiogenic sprouting has been widely reported (Davis et al., 2002). This process typically depends on the properties of the ECM, including its mechanical properties, sensitivity to cell-mediated degradation, and the presence of specific integrin-binding ligands (Browne and Healy, 2018). This process has been adopted as a strategy where ECs invade a collagen hydrogel and assemble into a complex vascular network (Vickerman et al., 2008) (Figure 2A). The role of shear flow and gradients of growth factors in vascular growth within the MPS have been investigated (Jeong et al., 2011; Shin et al., 2011). Similarly, these systems can assess drug effects and have been used to screen phthalimide derivates that were designed to maintain anti-angiogenic effects but reduced the teratogenicity that has been associated with phthalimide (Mercurio et al., 2019). Investigation into intricate cell-cell interactions, as well as creating more relevant disease models, can be achieved in tissues created in MPS via the inclusion of multiple compartments. In one instance, a device with multiple compartments was constructed to study the effect of Alzheimer disease on the BBB (Shin et al., 2019). Paracrine signals from Alzheimer disease neural progenitor cells (NPCs) compared with healthy NPCs increased the permeability of the BBB formed by ECs, while an increase in inflammatory markers was also detected. This emphasizes the effect of paracrine crosstalk rather than direct cell-cell contact since the two cell types were separated by multiple compartments. Two pharmacologic agents were tested for their capacity to recover the barrier function of the BBB, which etodolac was capable of doing, significantly enhancing the expression of Claudin-5 at the EC cell-cell junctions. Other examples of disease modeling include tumor cell intravasation across the vasculature. In one such study, the addition of macrophages to the MPS increased permeability, which was dependent on TNF-α (Zervantonakis et al., 2012). This impaired ECs

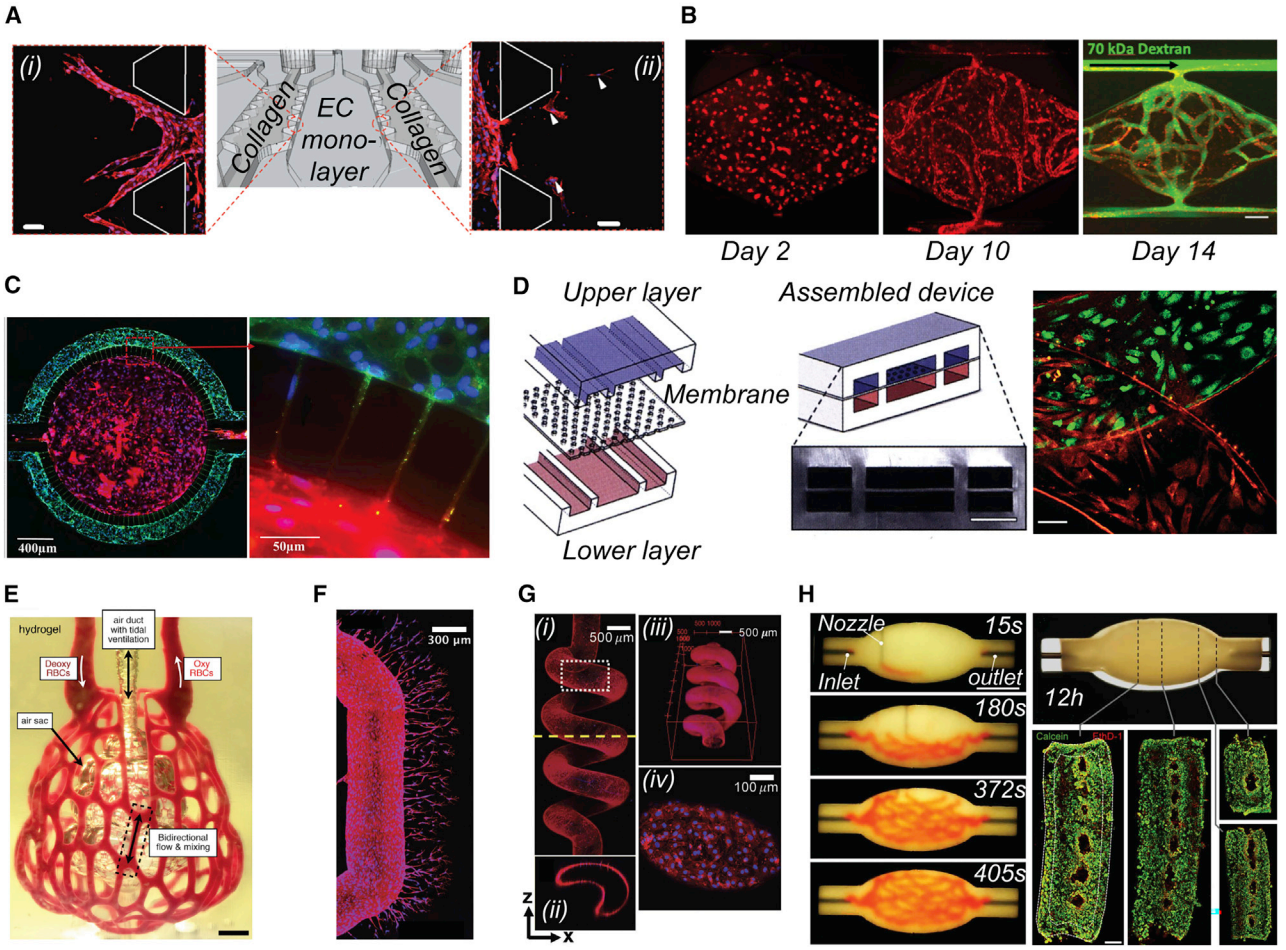

Figure 2. Representative images of vascularized microphysiological systems

(A) A quantitative microfluidic angiogenesis model, where endothelial cells migrate into the collagen chamber in response to VEGF gradient: (i) migration with VEGF, (ii) reduced migration with no VEGF. Scale represents 50 μm. Republished with permission of Royal Society of Chemistry, from Kim et al. (2014) .

(B) Vessel formation in fibrin gel in a microfluidic device tracked via mCherry-VE-cadherin. Physiological barrier function of the vascular network demonstrated via 70-kDa dextran (green) on day 14. Scale represents 50 μm. Republished with permission of Mary Ann Liebert inc. from Kurokawa et al. (2017) .

(C) A two-compartment blood-brain barrier MPS where the endothelial layer is separated from the tissue by microchannels. Vascular channel stained for ZO-1 (green), nuclei (blue), and astrocytes stained with astrocytic marker GFAP (red). Republished from Deosarkar et al. (2015) , permission through Creative Commons (CC).

(D) A tissue-tissue interface created by separating microfluidic channels by a porous polymeric membrane. Republished with permission from AAAS from Huh et al. (2010) . Endothelial cells (green) grown on one side of the membrane and vascular smooth muscle cells (red) on the other were used to study signaling between the two cell types. Scale represents 100 μm. Reproduced from Engeland et al. (2018) ; permission through CC-NC (non-commercial use).

(E and H) Representative images of biofabrication techniques for vascularized MPS. (E) Projection stereolithography used to create complex vascular geometry such as those seen in distal lung subunit. Scale represents 1 mm. Republished with permission from AAAS from Grigoryan et al. (2019) .

(F) Angiogenic sprouting from 3D printed channels into support hydrogel.

(G) Cell degradable hydrogels patterned using 3D fabrication technique to create spiral vasculature. Republished with permission of John Wiley and Sons Inc. from Song et al. (2018) .

(H) Time sequences of a vascularization of an embryoid body tissue. Viable cells at different sections of the tissue are shown stained green using live-dead assay. Scale on live-dead image represents 1 mm. Republished from Skylar-Scott et al. (2019) ; permission through CC-NC.

barrier function facilitated the enhanced transfer of tumor cells across the ECs barrier.

Similar approaches to model sprouting angiogenesis from existing vasculature have also been developed. This can involve polymerizing biopolymer-based hydrogels in the presence of needles that can then be withdrawn to create hollow channels of defined sizes (Nguyen et al., 2013), or by creating channels within biopolymer-based hydrogels using soft lithography. These channels may be endothelialized by seeding ECs within them, and used to study vascular sprouting into an ECM in response to gradients of angiogenic factors (Nguyen et al., 2013) or shear flow (Galie et al., 2014). In fact, this system identified 10 dyne/cm^2 as a threshold that activated angiogenic sprouting into a collagen matrix via an MMP-mediated mechanism. This approach was also used in combination with brain microvascular ECs derived from hiPSCs to model disruption of the BBB in response to treatment with the hyperosmotic agent mannitol (Linville et al., 2020). Transient increases in paracellular permeability through the formation of focal leaks were stimulated by mannitol exposure, which was followed by recovery of barrier function. A similar system, but in this case using a semi-synthetic dextran ECM, elucidated the importance of matrix crosslinking and degradation kinetics on sprouting (Trappmann et al., 2017), a phenomenon which has also been demonstrated *in vivo* (Jha et al., 2016). These systems can also be used to study the effect of ECs activation on adherence of platelets and leukocytes(Zheng et al., 2012). Addition of phorbol-12-myristate-13-acetate (PMA) stimulates the release and assembly of von Willebrand factor (vWF) into fibers that trap platelets and leukocytes from whole blood. This demonstrates the capacity of these systems to study both angiogenic sprouting and also the transition to a thrombogenic state during inflammation. Furthermore, the interaction between supporting SCs and ECs can be investigated by initially seeding a layer of SCs followed by a layer of ECs (Alimperti et al., 2017). This interaction between ECs and SCs enhanced barrier function, but stimulation with inflammatory mediators (lipopolysaccharide, thrombin, or TNF-α) enhanced permeability by stimulating support cells to detach from the vessel walls, a finding that was mimicked by *in vivo* studies. Using parallel vessels, the interaction between blood vessels and cancerous pancreatic ducts may also be elucidated. It was shown that cancerous pancreatic ducts grew toward channels lined with ECs and ablated the ECs (Nguyen et al., 2019). This was found to be dependent on the TGF-β pathway, as ECs could be rescued using SB431542, with further knockout studies implicating ALK7. Again, this finding was corroborated *in vivo*, emphasizing the power of the model.

An alternative approach involves the spontaneous assembly of a vascular network when ECs are encapsulated within an ECM, resembling vasculogenesis seen during development (Figure 2B). Loading of ECs, alongside supporting SCs, suspended within an ECM into an MPS allows for monitoring and repeated visualization of vascular network formation in a high-throughput manner. For example, Moya and co-workers (Phan et al., 2017) loaded endothelial colony-forming cell-derived ECs (ECFC-ECs) alongside FBs within a fibrin hydrogel that subsequently assembled into a perfusable network. This has also been demonstrated with hiPSC-ECs in a fibrin matrix, and also within a semi-synthetic growth factor sequestering hyaluronic acid (HyA) hydrogel system, with lumen patency demonstrated using fluorescent beads (Kurokawa et al., 2017; Natividad-Diaz et al., 2019). A similar system was used to study the effect of ionizing radiation on vascular networks, with clear differences observed between the 3D network and 2D studies with regard to adherens junction damage, apoptosis, and DNA damage and repair (Guo et al., 2019). These differences were attributed to the role of shear stress in the 3D network.

Basic mechanisms of tumor vascularization can also be studied within MPSs, such as the effect of cancer-associated fibroblasts (CAFs) on vasculogenesis. While the effect of soluble factors supporting angiogenesis is established, this study further elucidated the mechanical effect of CAFs on blood vessel formation in the tumor microenvironment (Sewell-Loftin et al., 2017). It was observed that CAFs supported vasculogenesis by the mechanical deformation of the ECM, while non-cancerous cells did not. Depletion of YAP signaling by CAFs reduced vasculogenesis, further supporting the hypothesis that mechanotransduction plays a role in tumor vascularization. Furthermore, vascularization could be partially recovered by mechanical perturbation of the matrix using magnetic beads. Addition of more chambers in the MPS allowed investigating interactions between quiescent vasculature and tumors, including the effect of anti-angiogenic drugs and the ability of tumor cells to cross the basement membrane into adjacent vasculature (Sobrino et al., 2016). Demonstrated differences in the growth and invasion between differentially aggressive tumor lines in the MPS emphasizes the power of using a patient-derived tumor on chip for personalized medicine.

Given that the sprouting and self-assembly of ECs will depend heavily on the properties of the ECM, the choice of ECM is of major significance. Examples described above typically use well-established natural biopolymers such as collagen and fibrin as the base ECM, although modified biopolymers or synthetic matrices may also be used. For example, a study using hiPSC-ECs in a poly(ethylene glycol) (PEG)-based hydrogel demonstrated the importance of swelling for vascularization in a confined volume (Brown et al., 2020). It was observed that, in conventional

cell culture, a free-swelling PEG-based hydrogel could support vascular network formation by hiPSC-ECs, but the same hydrogel could not in the confined geometry of an MPS. The inclusion of a PEG-grafted poly(propargyl-L-glutamate) resulted in neutral swelling properties and supported vascular network formation in a confined MPS environment. While this issue does not appear to be an issue with natural ECM-derived materials, modification of surfaces with PLL to prevent retraction of collagen hydrogels from the MPS wall improved the physiological growth of ECs into the matrix (Chung et al., 2009). These studies emphasize the important role materials science has to play in the development of MPSs, and particularly the challenge of faithfully recapitulating physiological vascular networks and vascularization.

Engineered interfaces

The tissue interface between the ECs and the perivascular/parenchymal cells can be modeled via engineered structures that act as a barrier between the two cellular compartments. Designs using microchannels or a grid of microgrooves have been proposed in order to create an interface between a vascular and tissue compartment (Figure 2C) (Deosarkar et al., 2015; Yeste et al., 2017). However, the most commonly used design for creating tissue-tissue interfaces includes two microfluidic channels separated by a polymer membrane, where the ECs are seeded on one side while perivascular/parenchymal cell of interest is cultured directly on the opposite side of the membrane (Figure 2D). The separation of the fluidic channels with a membrane allows the provision of appropriate shear stress to the ECs while protecting the parenchyma from deleterious effects of shear. The porous microstructure of the polymeric membrane enables the paracrine communication between the ECs and the tissue of interest. These MPS also facilitate the inclusion of biophysical cues such as fluid flow and cyclic mechanical deformations, which are vital for accurately emulating functional units of human organs. This microfluidic device strategy has been used to model multiple tissue interfaces such as the BBB (Park et al., 2019), lung alveoli (Benam et al., 2016), the kidney glomerulus (Musah et al., 2017), and the intestinal villi (Vatine et al., 2019). Establishment of reliable tissue MPS models, which account for drug absorption losses into the external casing of the MPS, have led to obtaining more detailed and physiological pharmacokinetics of drugs compared with *in vivo* models (Herland et al., 2020; Lee-Montiel et al., 2020; Reese et al., 2020; Yu et al., 2015).

The spatial separation of the parenchymal tissue and the vascular channels offers the unique possibility to elucidate the role of the vasculature in the respective organ by comparing the functionality of the tissue cultured in the microfluidic device either with or without an endothelial lining. For example, the role of the endothelium in the endometrium during reproductive processes was recently explored using a barrier MPS (Gnecco et al., 2019). It was shown that the differentiation of stromal FBs into the decidua of the placenta is promoted via paracrine signals from ECs, an essential process in pregnancy. ECs in the MPS secreted prostaglandin E2 and prostacyclin via the shear stress-induced COX-2 pathway, which mediated the progestin-driven stromal differentiation. No difference in stromal differentiation into the decidua was observed when comparing monoculture of SCs and static co-culture conditions. The application of the appropriate shear force to the endothelial lining to regulate their paracrine signaling function emphasizes one of the key advantages of MPSs including tissue interfaces over traditional 2D culture systems.

Apart from investigating the contribution of ECs for the normal function of healthy tissues, barrier-based MPS provide a valuable tool for studying the function of ECs in disease. For example, Benam et al. (2016) observed that the human pulmonary endothelium contributes significantly to viral-induced pulmonary inflammation using a barrier-based microfluidic device. In this model, exposure to viral mimic polyinosinic-polycytidylic acid increased the secretion of the proinflammatory cytokines chemokine (C-C motif) ligand 5 (CCL5), IL-6, and C-X-C motif chemokine ligand 10 by at least 3-fold when an interface between ECs and airway epithelial cells was created compared with the epithelium cultured alone. Neutrophil recruitment was shown to increase upon the upregulation of E-selectin and VCAM-1 in the endothelial layer when stimulated with the viral mimic. Role of the ECs in different pathologies, such as cancer and pulmonary thrombosis, have been explored using this MPS strategy (Jain et al., 2018; Morad et al., 2019).

The endothelium's vital role in various tissue processes has also been recognized by linking multiple MPS tissue compartments or organs on a chip together. A fluidically connected multi-MPS, in which each MPS represents a specific part of a tissue, was used to investigate the metabolic interaction between the BBB and the brain parenchymal tissue (Maoz et al., 2018). It was observed that vascular metabolites that are produced by the ECs and/or the perivascular cells of the BBB chip directly influence the synthesis of gamma aminobutyric acid (GABA), an important neurotransmitter, by the neural cells cultured in the fluidically connected brain chip. Such findings and approach can be useful to answer mechanistic questions aimed at the link between neuro-metabolism and neuro-pathologies.

The aforementioned examples highlighted the use of primary cells; however, the use of cells differentiated from hiPSCs opens the path for engineered barrier interface strategies to develop disease model MPS. For example, isogenic model of Huntington disease and brain EC monocarboxylate

8 deficiency have been emulated in these MPSs (Vatine et al., 2019). In the same study, hemodynamic force on the ECs, exerted by the fluid flow, was shown to mature the hiPSC-derived brain microvascular ECs cultured in a BBB MPS. Flow-dependent increases in the expression of endothelial markers (such as occludin, CD31, and vWF) in hiPSC brain microvascular ECs were observed. Furthermore, expression of pathways that are related to BBB maturation, metabolism, and vascular functions were enhanced with shear stress. Barrier function was observed to improve when co-cultured with isogenic hiPSC-derived neural cells as determined by a decrease in permeability to dextran molecules.

A recent article proposed that these MPS microfluidic cultures serve as better alternatives to organoid systems in achieving functional maturity due to better incorporation of physiologically relevant biophysical cues to both the ECs and the epithelium. For example, Kasendra et al. (2018) used primary human intestinal epithelial cells derived from organoids established from the duodenum tissue and tissue-specific primary microvascular ECs in a co-culture system in the MPS, applying cyclic strain and fluid flow to the tissues. Transcriptomic comparison between the intestine MPS, organoids, and *in vivo* extracts of the human duodenum revealed that the MPS resembled the phenotype and gene expression of the *in vivo* duodenum closer than a conventional organoid culture that does not include an endothelium and mechanical stimulation.

The integration of an endothelial lining as well as biophysical cues has been used to improve the functional maturity of hiPSC-derived tissues in MPS. For example, tissue-specific primary human glomerular microvascular ECs induced the functional maturation of hiPSC-derived podocytes when cultured on either side of a porous membrane in a microfluidic device, while also being subjected to fluid flow and mechanical strain (Musah et al., 2017). Matured podocytes secreted 2-fold VEGF-A, a known growth factor for vascular patterning in glomeruli *in vivo*, compared with podocytes co-cultured under static conditions. Co-cultured podocytes also demonstrated differential urinary clearance of albumin and inulin that mimicked *in vivo* clearance rates. Furthermore, this *in vitro* MPS closely simulated kidney injury induced by cancer drug doxorubicin, as noted by the dose-dependent delamination of podocytes and decreased viability, and loss of barrier function to albumin.

As one of the main functions of the endothelial lining in the vasculature is to provide a selective barrier, interface-based MPS with separate compartments represent a unique model to study drug transport in hiPSC-based models. Park et al. (2019) demonstrated an MPS representing the BBB consisting of hiPSC-EC, co-cultured with primary human astrocytes and pericytes, that could maintain higher (>2.5 fold compared with an equivalent 2D transwell system) barrier function for 7 days as measured by TEER measurements. Notably, the combination of a better differentiation protocol for the hiPSC-ECs and microfluidic culture allowed this study to recapitulate the *in vivo* interaction of P-glycoprotein, a critical barrier protein, and the antidepressant drug citalopram. Such interactions could not be reproduced in 2D *in vitro* models incorporating non-human cells, highlighting the advantage of using hiPSC-derived cells in combination with MPS.

Recent developments include incorporation of integrated sensors (such as TEER) and even MPS modules that can be reused (Yeste et al., 2017). However, it should be noted that choice of membrane material and physical properties needs to be taken into consideration when trying to model a vascularized tissue. Typical materials used for the membranes include poly(dimethyl siloxane), poly(carbonate), poly(ethylene terephthalate), poly(lactic acid), and poly(ε-caprolactone). The material properties such as surface roughness, hydrophilicity, mechanical stiffness, and porosity influence cell attachment and behavior (Casillo et al., 2017). For example, polymer micropore density influences cell-cell and cell-substrate interactions, which therefore controls the amount of shear stress that may be introduced into the fluidic channels without the loss of the EC layer (Salminen et al., 2019). This may limit the amount of shear stress that can be provided to the ECs in the membrane-based barrier MPS.

Advances in 3D vascular biofabrication

Biofabrication is an evolving definition referring to automated manufacturing technologies that create functional biological products from cells and bioactive materials, encompassing 3D printing (Figures 2E–2H). They offer attractive prospects for developing vascular MPS given their ability to robotically assemble a broad range of materials in sophisticated geometries and compositions, in some cases using multiple printing techniques and assembling multi-component devices. Increasingly the research focus has shifted to post-printed functionality, ranging from operational printed electrodes to prompting aspects of tissue maturation (Levato et al., 2020). Relating to vascular MPS, this includes cell-laden constructs that demonstrate vessel structure and behavior, and realistic responsiveness to perfused drugs and angiogenic stimuli. Thematically, strategies used in biofabrication to create vessel structures include casting hydrogel matrices around printed sacrificial channels (Kolesky et al., 2016; Miller et al., 2012), printing channels within a support bath (Hinton et al., 2015; Song et al., 2018), stereolithography based techniques (Grigoryan et al., 2019; Song et al., 2018), and photoablation/multi-photon approaches (Arakawa et al., 2017).

Printing bioinks within a support bath maintains hydration during assembly of complex structures that require

lengthy, intricate patterning and provides support to bioinks with non-instantaneous crosslinking mechanisms. Microporous collagen scaffolds were created through incorporating sacrificial gelatin microparticles within pre-gelled collagen and FRESH (freeform reversible embedding of suspended hydrogels; Hinton et al., 2015) bioprinting. The microporosity created by this 3D bioprinting strategy significantly improved cell infiltration, stimulating *in vivo* microvascular integration (Lee et al., 2019). Similarly, hollow lumens lined with hiPSC-ECs were patterned within cardiac patches formed of hiPSC-derived cardiomyocytes encased in a decellularized human omentum tissue ECM bioink (Noor et al., 2019). *In vitro* studies demonstrated tissue several millimeters thick with perfusable vessel structures, and contractile functionality was measured by calcium transients.

Combinations of support bath-based bioprinting strategies with projection stereolithography (Grigoryan et al., 2019) and synthetic hydrogels (Song et al., 2018) have been used to push the boundaries of complex microchannel geometry (Figures 2E–2G). Complex vascular geometry and fluid mixing regimes were recently created with such an approach, demonstrating models of red blood cell perfusion and alveolar topography (Grigoryan et al., 2019). This plays to the strengths of 3D printing as elaborate, entangled microchannels such as this would not be possible with conventional soft lithography. Another topical example reported innovative support hydrogel chemistry that utilized thiol-based crosslinking to integrate RGD cell adhesion peptides and protease-sensitive degradation (Song et al., 2018). The modifications to the support hydrogel enabled HUVECs to demonstrate angiogenic sprouting toward perfused growth factors. Comparable angiogenic sprouting assays in PDMS-cast MPS typically rely on micropillars to tune cellular invasion, which impose geometric restrictions on angiogenic outgrowth. Another synthetic chemistry-driven approach designed a photodegradable hydrogel that was subtractively patterned with multiphoton lithography to create rounded microchannels with widths in the range of 10–200 μm (Arakawa et al., 2017). In this configuration the support hydrogel encapsulated bone-marrow-derived human SCs and post-fabrication the channels were seeded with HUVECs.

Replicating vessel permeability and interaction with surrounding cells has been a key focus of several other strategies. A novel 3D stamping technique was used to create branched 3D microchannel networks, with HUVECs-lined lumens surrounded by ECM and tissue-specific cells (primary or ESC-derived hepatocytes and cardiomyocytes) and mesenchymal stem cells (MSCs) (Zhang et al., 2016a). The scaffold was designed to impart mechanical reinforcement for surgical anastomosis and had surface micro- and nanopores to tune vascular permeability and crosstalk between cell types. Notably, angiogenic sprouting could be stimulated with thymosin β4 and perfusion with whole blood led to monocyte migration across the endothelial barrier. A co-axial nozzle configuration was used to create fast-gelling HUVECs-laden alginate-gelatin methacryloyl (GelMA) fibers (Zhang et al., 2016b). Post-printing, the embedded HUVECs migrated to the fiber surface forming an endothelium and subsequent seeding with cardiomyocytes created an aligned myocardium model capable of spontaneous and synchronized contractile function. The printed construct was integrated into a custom perfusion bioreactor and further studies were completed with hiPSC-derived cardiomyocytes. Both cardiomyocytes and ECs displayed dose-dependent responses to doxorubicin, assessed by beat rate and vWF secretion respectively, showing correlation with murine controls and 2D studies.

Co-axial extrusion systems have also been used to create perfusable vessel models without an external matrix. One example embedded HUVECs within a hollow structure of decellularized ECM alginate (Gao et al., 2018). Maturity of the endothelial lining was characterized by expression of VE cadherin; ki-67 expression on day 0 and 7 as a mesaure of quiescence; and, deposition of laminin. ECs aligned with the fluid flow, upregulating SMAD6, SMAD7, KLF2, and eNOS expression: characteristics relating to TGF-β signaling regulation, EC survival, and physiological conditions. The system demonstrated angiogenic sprouting toward external VEGF and bFGF, and responsiveness to inflammatory cytokines generated from stimulated airway epithelial cells. Angiogenic instability was attributed to the lack of perivascular cells, indicating a future research direction. Another recent co-axial extrusion study had a core of Matrigel laden with HUVECs and SMCs, sheathed by alginate (Andrique et al., 2019). Within a day, the cells self-assembled into distinct cellular layers with HUVECs lining the lumen. The printed vesseloid constructs were perfusable, measured cell quiescence via ki-67 and caspase-3 expression; physiological barrier function through dextran perfusion and transmission electron microscopy imaging of cell junctions, and contractility in response to vasoconstrictor agents. Cell-free and HUVECs monoculture controls validated the biofunctionality achieved by mural co-culture.

Significant advances have also been made using sacrificial micromolding techniques with vascular stromal co-culture. This allows a cell-laden matrix to be cast around a temporary branched structure, which may be removed by temperature changes or solubilization, templating a microchannel network for subsequent endothelialization. Recently this approach was applied with selective laser sintering to create complicated dendritic vascular networks as a sacrificial template (Kinstlinger et al., 2020). Pluronic-based sacrificial inks have been used to build viable

in vitro tissues that were a centimeter thick for prolonged culture (Kolesky et al., 2016). MSCs and FBs embedded in the support matrix migrated to the endothelialized channels and adopted pericyte-like behaviors depositing collagen I and stabilizing the lumen structure. This method was recently developed for printing gelatin-based sacrificial channels directly in a bath of cell aggregates or brain organoids (Figure 2H), obtaining a much higher cellular density (Skylar-Scott et al., 2019). There has been some investigation of crosstalk between different tissues (Lin et al., 2019). One study assessed albumin and glucose reabsorption utilizing human proximal tubule epithelial cells and glomerular microvascular ECs. Induced hyperglycemic conditions investigated endothelial dysfunction and responsivity to the renal drug dapagliflozin in contrast to non-elevated glucose levels.

3D bioprinting strategies can offer complex patterning capabilities, although much of the aforementioned literature avoids directly printing cells. To reduce cell death due to shear stress or lengthy fabrication procedures, many opt to seed cells on printed structures or print around them, rather than direct embedding. For some structures, a more simple and rapid assembly process may be preferable, such as hydrogel casting. In addition, bioprinted materials face conflicting structural demands. If insufficient, a structure may not be able to support its own weight and desired cellular organization. However, non-physiological stiffness can suppress cell outgrowth and tissue remodeling processes such as angiogenic sprouting. HUVECs have been a predominant cell source used for vascularization research, with limited studies employing hiPSC- and ESC-derived ECs. Established 3D printing technologies are becoming sufficiently robust to model greater biological organization and complexity, such as hiPSC-ECs alongside SCs (Noor et al., 2019) or with tissue specificity (Lin et al., 2019). Equally, combining hiPSC technology, advances in 3D biofabrication and MPS allows for sophisticated tissue organization and the modeling of physical stimuli such as shear flow.

Future directions and perspective

Development of stem cell-derived and tissue-specific vasculature has the potential to more accurately recapitulate tissue functionality and transport mechanisms in MPS. However, the source of cells to vascularize MPS deserves careful consideration. Across tissue and vessel type (artery, capillary, vein, and lymphatics) ECs demonstrate considerable heterogeneity, as has been recently demonstrated with single-cell RNA sequencing (scRNA-seq) (Kalucka et al., 2020). This analysis revealed tissue type, rather than vessel type, predominantly contributed to the heterogeneity of ECs. Similarly for SCs, FBs demonstrate distinct gene expression profiles dependent on anatomical location (LeBleu and Neilson, 2020). However, most MPS technologies have relied heavily on primary cells and cell lines such as HUVECs for vascularization, and some include perivascular and stromal cell types, although often without tissue or species specificity. While primary cells provide valuable insight and can impart tissue specificity, batch-to-batch variation and the use of cells of different genetic backgrounds or species complicates interpretations derived from MPSs. In particular, interactions between immune cells and vasculature of differing genetic backgrounds or species could cloud immune responses and lead to confounding data. Progress in hiPSC/PSC technology has allowed investigators to overcome these challenges and has opened up the possibility of generating isogenic tissue models, eliminating non-self-immune responses. Furthermore, protocols have been developed to derive tissue-specific ECs and SCs from hiPSCs, most notably cells of the BBB (Neal et al., 2019; Stebbins et al., 2019). The choice of SCs has been shown to be important when engineering cardiac tissues (Hookway et al., 2019); additionally, CAFs have been shown to enhance angiogenesis in MPSs via increased mechanical strain on the ECM compared with non-cancerous FBs (Sewell-Loftin et al., 2020). Cardiac microtissues composed of cardiomyocytes, cardiac ECs, and cardiac FBs, all of hiPSC origin, were recently reported, displaying enhanced functional maturity compared with a reference with primary skin fibroblasts instead of cardiac hiPSC-FBs (Giacomelli et al., 2020). The microtissues with cardiac-specific FBs exhibited more complex microstructure, enhanced contractility, and more mature electrophysiology. These examples highlight the need to select cell sources that account for tissue and disease specificity when developing representative vasculature within MPS. Combined with biophysical and biochemical cues presented in MPSs that mimic the native tissue niche, aspects of tissue specificity are attainable. This could involve coculture with parenchymal cells, physiological shear flow, or the introduction of tissue-mimetic ECM features, as depicted in Figure 3.

Despite their undoubted potential for drug discovery and disease modeling, the maturity of hiPSC/PSC-derived cells remains a challenge (Tiemeier et al., 2019), while the loss of physiological phenotype and functionality in 2D culture could limit scale-up. This review points to the utility of MPS in improving the maturity of both the parenchyma and the vasculature, often attributed to complementary crosstalk between cellular niches. Use of scRNA-seq to contrast *in vivo* EC phenotypes and pericyte plasticity with those established within MPSs to existing *in vitro* systems could be a worthwhile pursuit (Guimarães-Camboa et al., 2017). Additionally, hiPSC/PSC-derived MPS models present challenges in the maintenance of long-term experiments depending on the choice of culture media and the fluidics

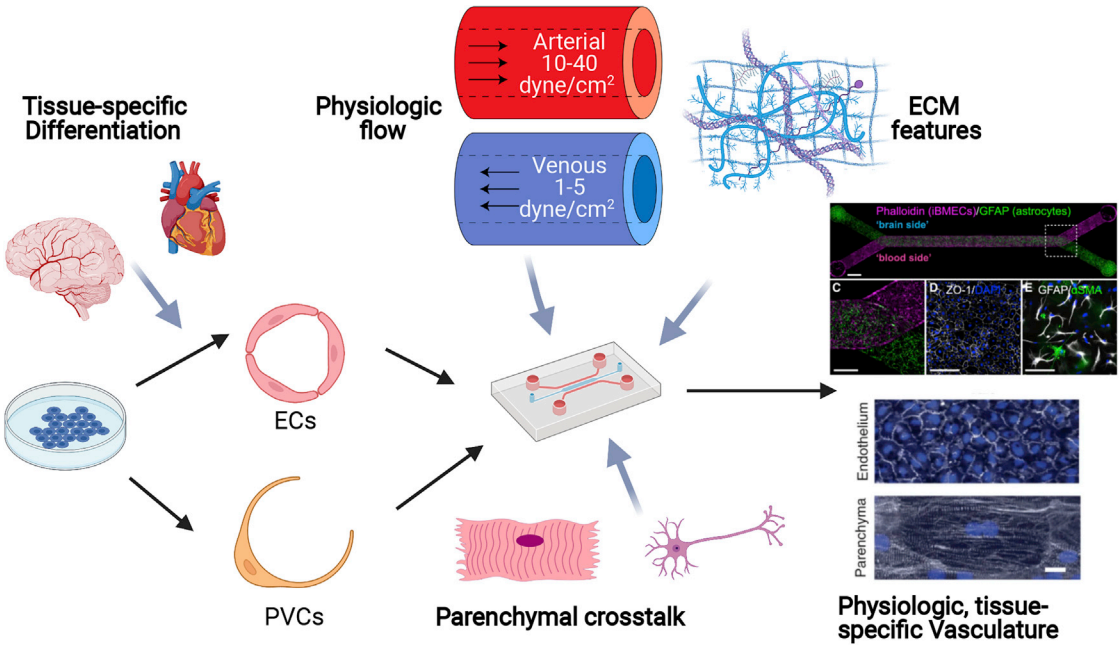

Figure 3. Development of physiological, and tissue specific vasculature in MPSs

A schematic representation of the approaches that may be used to develop vascularized MPSs, including using tissue-specific differentiation protocols, and incorporating signals such as physiological flow, ECM features, and parenchymal cells. Images republished from Vatine et al. (2019) , with permission from Elsevier, and Novak et al. (2020) with permission from Springer Nature. Scale bars represent 1mm, 500 μm, 200 μm, 100 μm, and 100 μm for republished images from left to right, going downward. Figure created with BioRender.com.

used in the MPS to feed the tissue (i.e., separate media supplied for different cells or common media). Addressing these challenges will open more avenues to explore the synergistic coupling of MPS and hiPSC technologies to create biologically relevant and predictive models. Isogenic models of rare diseases such as Hutchinson-Gilford progeria syndrome and Huntington disease have now been realized using combined MPS-hiPSC technology (Atchison et al., 2020; Vatine et al., 2019), thus highlighting the potential for personalized medicine to capture the diversity of genetic backgrounds for drug discovery and/or development. A focus on personalized vascular models is also timely for investigating patient responses to coronavirus disease 2019 (COVID-19) and assessing novel therapeutics, since viral infection of ECs and resulting cardiovascular complications have been established as contributors to COVID-19 pathophysiology (Teuwen et al., 2020; Varga et al., 2020). The development of microfluidic MPS models has to be parallel with the development of assays optimized for microfluidic handling and allowing the collection of accurate and quantitative data.

The integration of vasculature within MPSs is a multidisciplinary problem, requiring expertise in stem cell biology, materials science, and engineering. Realizing the potential of organ-specific vasculature derived from hiPSCs within MPSs will allow for more informative and precise models to study basic biological mechanisms, transport phenomena, and disease modeling to screen promising therapeutics.

DECLARATION OF INTERESTS

The authors have no financial interests to declare.

REFERENCES

Alimperti, S., Mirabella, T., Bajaj, V., Polacheck, W., Pirone, D.M., Duffield, J., Eyckmans, J., Assoian, R.K., and Chen, C.S. (2017). Three-dimensional biomimetic vascular model reveals a RhoA, Rac1, and *N*-cadherin balance in mural cell–endothelial cell-regulated barrier function. Proc. Natl. Acad. Sci. U S A *114*, 8758–8763.

Andrique, L., Recher, G., Alessandri, K., Pujol, N., Feyeux, M., Bon, P., Cognet, L., Nassoy, P., and Bikfalvi, A. (2019). A model of guided cell self-organization for rapid and spontaneous formation of functional vessels. Sci. Adv. *5*, eaau6562.

Arakawa, C.K., Badeau, B.A., Zheng, Y., and DeForest, C.A. (2017). Multicellular vascularized engineered tissues through user-programmable biomaterial photodegradation. Adv. Mater. *29*. 10.1002/adma.201703156.

Atchison, L., Abutaleb, N.O., Snyder-Mounts, E., Gete, Y., Ladha, A., Ribar, T., Cao, K., and Truskey, G.A. (2020). iPSC-derived endothelial cells affect vascular function in a tissue-engineered blood

vessel model of Hutchinson-Gilford progeria syndrome. Stem Cell Rep. *14*, 325–337.

Augustin, H.G., and Koh, G.Y. (2017). Organotypic vasculature: from descriptive heterogeneity to functional pathophysiology. Science *357*, eaal2379.

Benam, K.H., Villenave, R., Lucchesi, C., Varone, A., Hubeau, C., Lee, H.-H., Alves, S.E., Salmon, M., Ferrante, T.C., Weaver, J.C., et al. (2016). Small airway-on-a-chip enables analysis of human lung inflammation and drug responses in vitro. Nat. Methods *13*, 151–157.

Brown, A., He, H., Trumper, E., Valdez, J., Hammond, P., and Griffith, L.G. (2020). Engineering PEG-based hydrogels to foster efficient endothelial network formation in free-swelling and confined microenvironments. Biomaterials *243*, 119921.

Browne, S., and Healy, K.E. (2018). Matrix-assisted cell transplantation for tissue vascularization. Adv. Drug Deliv. Rev. *146*, 155–169.

Browne, S., Jha, A.K., Ameri, K., Marcus, S.G., Yeghiazarians, Y., and Healy, K.E. (2018). TGF-β1/CD105 signaling controls vascular network formation within growth factor sequestering hyaluronic acid hydrogels. PLoS One *13*, e0194679.

Casillo, S.M., Peredo, A.P., Perry, S.J., Chung, H.H., and Gaborski, T.R. (2017). Membrane pore spacing can modulate endothelial cell–substrate and cell–cell interactions. ACS Biomater. Sci. Eng. *3*, 243–248.

Chatterjee, S., and Fisher, A.B. (2014). Mechanotransduction in the endothelium: role of membrane proteins and reactive oxygen species in sensing, transduction, and transmission of the signal with altered blood flow. Antioxid. Redox Signal. *20*, 899–913.

Cheung, C., Bernardo, A.S., Trotter, M.W.B., Pedersen, R.A., and Sinha, S. (2012). Generation of human vascular smooth muscle subtypes provides insight into embryological origin–dependent disease susceptibility. Nat. Biotechnol. *30*, 165–173.

Chung, A.S., and Ferrara, N. (2011). Developmental and pathological angiogenesis. Annu. Rev. Cell Dev. Biol. *27*, 563–584.

Chung, S., Sudo, R., Zervantonakis, I.K., Rimchala, T., and Kamm, R.D. (2009). Surface-treatment-induced three-dimensional capillary morphogenesis in a microfluidic platform. Adv. Mater. *21*, 4863–4867.

Coppiello, G., Collantes, M., Sirerol-Piquer, M.S., Vandenwijngaert, S., Schoors, S., Swinnen, M., Vandersmissen, I., Herijgers, P., Topal, B., van Loon, J., et al. (2015). Meox2/Tcf15 heterodimers program the heart capillary endothelium for cardiac fatty acid uptake. Circulation *131*, 815–826.

Cui, X., Lu, Y.W., Lee, V., Kim, D., Dorsey, T., Wang, Q., Lee, Y., Vincent, P., Schwarz, J., and Dai, G. (2015). Venous endothelial marker COUP-TFII regulates the distinct pathologic potentials of adult arteries and veins. Sci. Rep. *5*, 16193.

Davis, G.E., Bayless, K.J., and Mavila, A. (2002). Molecular basis of endothelial cell morphogenesis in three-dimensional extracellular matrices. Anat. Rec. *268*, 252–275.

Deosarkar, S.P., Prabhakarpandian, B., Wang, B., Sheffield, J.B., Krynska, B., and Kiani, M.F. (2015). A novel dynamic neonatal blood-brain barrier on a chip. PLoS One *10*, e0142725.

Engeland, N.C.A.van, Pollet, A.M.A.O., Toonder, J.M.J.den, Bouten, C.V.C., Stassen, O.M.J.A., and Sahlgren, C.M. (2018). A biomimetic microfluidic model to study signalling between endothelial and vascular smooth muscle cells under hemodynamic conditions. Lab Chip *18*, 1607–1620.

Gadue, P., Huber, T.L., Paddison, P.J., and Keller, G.M. (2006). Wnt and TGF-ß signaling are required for the induction of an in vitro model of primitive streak formation using embryonic stem cells. Proc Natl Acad Sci U S A *103*, 16806–16811.

Gaengel, K., Genové, G., Armulik, A., and Betsholtz, C. (2009). Endothelial-mural cell signaling in vascular development and angiogenesis. ATVB *29*, 630–638.

Galie, P.A., Nguyen, D.-H.T., Choi, C.K., Cohen, D.M., Janmey, P.A., and Chen, C.S. (2014). Fluid shear stress threshold regulates angiogenic sprouting. Proc. Natl. Acad. Sci. *111*, 7968–7973.

Gao, G., Park, J.Y., Kim, B.S., Jang, J., and Cho, D.-W. (2018). Coaxial cell printing of freestanding, perfusable, and functional in vitro vascular models for recapitulation of native vascular endothelium pathophysiology. Adv. Healthc. Mater. *7*, 1801102.

Giacomelli, E., Meraviglia, V., Campostrini, G., Cochrane, A., Cao, X., van Helden, R.W.J., Krotenberg Garcia, A., Mircea, M., Kostidis, S., Davis, R.P., et al. (2020). Human-iPSC-derived cardiac stromal cells enhance maturation in 3D cardiac microtissues and reveal non-cardiomyocyte contributions to heart disease. Cell Stem Cell *26*, 862–879.e11.

Gnecco, J.S., Ding, T., Smith, C., Lu, J., Bruner-Tran, K.L., and Osteen, K.G. (2019). Hemodynamic forces enhance decidualization via endothelial-derived prostaglandin E2 and prostacyclin in a microfluidic model of the human endometrium. Hum. Reprod. *34*, 702–714.

Granata, A., Serrano, F., Bernard, W.G., McNamara, M., Low, L., Sastry, P., and Sinha, S. (2017). An iPSC-derived vascular model of Marfan syndrome identifies key mediators of smooth muscle cell death. Nat. Genet. *49*, 97–109.

Grigoryan, B., Paulsen, S.J., Corbett, D.C., Sazer, D.W., Fortin, C.L., Zaita, A.J., Greenfield, P.T., Calafat, N.J., Gounley, J.P., Ta, A.H., et al. (2019). Multivascular networks and functional intravascular topologies within biocompatible hydrogels. Science *364*, 458–464.

Guimarães-Camboa, N., Cattaneo, P., Sun, Y., Moore-Morris, T., Gu, Y., Dalton, N.D., Rockenstein, E., Masliah, E., Peterson, K.L., Stallcup, W.B., et al. (2017). Pericytes of multiple organs do not behave as mesenchymal stem cells in vivo. Cell Stem Cell *20*, 345–359.e5.

Guo, Z., Yang, C., Maritz, M.F., Wu, H., Wilson, P., Warkiani, M.E., Chien, C., Kempson, I., Aref, A.R., and Thierry, B. (2019). Validation of a vasculogenesis microfluidic model for radiobiological studies of the human microvasculature. Adv. Mater. Technol. *4*, 1800726.

Halaidych, O.V., Cochrane, A., van den Hil, F.E., Mummery, C.L., and Orlova, V.V. (2019). Quantitative analysis of intracellular Ca2+ release and contraction in hiPSC-derived vascular smooth muscle cells. Stem Cell Rep. *12*, 647–656.

Harding, A., Cortez-Toledo, E., Magner, N.L., Beegle, J.R., Coleal-Bergum, D.P., Hao, D., Wang, A., Nolta, J.A., and Zhou, P. (2017). Highly efficient differentiation of endothelial cells from pluripotent stem cells requires the MAPK and the PI3K pathways: the

MAPK and PI3K pathways in endothelial fate. Stem Cells *35*, 909–919.

Herland, A., Maoz, B.M., Das, D., Somayaji, M.R., Prantil-Baun, R., Novak, R., Cronce, M., Huffstater, T., Jeanty, S.S.F., Ingram, M., et al. (2020). Quantitative prediction of human pharmacokinetic responses to drugs via fluidically coupled vascularized organ chips. Nat. Biomed. Eng. *4*, 421–436.

Hinton, T.J., Jallerat, Q., Palchesko, R.N., Park, J.H., Grodzicki, M.S., Shue, H., Ramadan, M.H., Hudson, A.R., and Feinberg, A.W. (2015). Three-dimensional printing of complex biological structures by freeform reversible embedding of suspended hydrogels. Sci. Adv. *1*, 1–10.

Hookway, T.A., Matthys, O.B., Mendoza-Camacho, F.N., Rains, S., Sepulveda, J.E., Joy, D.A., and McDevitt, T.C. (2019). Phenotypic variation between stromal cells differentially impacts engineered cardiac tissue function. Tissue Eng. A *25*, 773–785.

Huh, D., Matthews, B.D., Mammoto, A., Montoya-Zavala, M., Hsin, H.Y., and Ingber, D.E. (2010). Reconstituting organ-level lung functions on a chip. Science *328*, 1662–1668.

Isidori, A.M., Venneri, M.A., and Fiore, D. (2016). Angiopoietin-1 and angiopoietin-2 in metabolic disorders: therapeutic strategies to restore the highs and lows of angiogenesis in diabetes. J. Endocrinol. Invest. *39*, 1235–1246.

Jain, R.K. (2003). Molecular regulation of vessel maturation. Nat. Med. *9*, 685–693.

Jain, A., Barrile, R., van der Meer, A., Mammoto, A., Mammoto, T., Ceunynck, K.D., Aisiku, O., Otieno, M.A., Louden, C.S., Hamilton, G.A., et al. (2018). Primary human lung alveolus-on-a-chip model of intravascular thrombosis for assessment of therapeutics. Clin. Pharmacol. Ther. *103*, 332–340.

Jeong, G.S., Han, S., Shin, Y., Kwon, G.H., Kamm, R.D., Lee, S.-H., and Chung, S. (2011). Sprouting angiogenesis under a chemical gradient regulated by interactions with an endothelial monolayer in a microfluidic platform. Anal. Chem. *83*, 8454–8459.

Jha, A.K., Tharp, K.M., Browne, S., Ye, J., Stahl, A., Yeghiazarians, Y., and Healy, K.E. (2016). Matrix metalloproteinase-13 mediated degradation of hyaluronic acid-based matrices orchestrates stem cell engraftment through vascular integration. Biomaterials *89*, 136–147.

Kalucka, J., de Rooij, L.P.M.H., Goveia, J., Rohlenova, K., Dumas, S.J., Meta, E., Conchinha, N.V., Taverna, F., Teuwen, L.-A., Veys, K., et al. (2020). Single-cell transcriptome atlas of murine endothelial cells. Cell *180*, 764–779.e20.

Kasendra, M., Tovaglieri, A., Sontheimer-Phelps, A., Jalili-Firoozinezhad, S., Bein, A., Chalkiadaki, A., Scholl, W., Zhang, C., Rickner, H., Richmond, C.A., et al. (2018). Development of a primary human small intestine-on-a-chip using biopsy-derived organoids. Sci. Rep. *8*, 2871.

Kim, C., Kasuya, J., Jeon, J., Chung, S., and Kamm, R.D. (2014). A quantitative microfluidic angiogenesis screen for studying anti-angiogenic therapeutic drugs. Lab Chip *15*, 301–310.

Kim, Y., Park, N., Rim, Y.A., Nam, Y., Jung, H., Lee, K., and Ju, J.H. (2018). Establishment of a complex skin structure via layered co-culture of keratinocytes and fibroblasts derived from induced pluripotent stem cells. Stem Cell Res. Ther. *9*, 1–10.

Kinstlinger, I.S., Saxton, S.H., Calderon, G.A., Ruiz, K.V., Yalacki, D.R., Deme, P.R., Rosenkrantz, J.E., Louis-Rosenberg, J.D., Johansson, F., Janson, K.D., et al. (2020). Generation of model tissues with dendritic vascular networks via sacrificial laser-sintered carbohydrate templates. Nat. Biomed. Eng. *4*, 916–932.

Kolesky, D.B., Homan, K.A., Skylar-Scott, M.A., and Lewis, J.A. (2016). Three-dimensional bioprinting of thick vascularized tissues. Proc. Natl. Acad. Sci. U S A *113*, 3179–3184.

Kumar, A., D'Souza, S.S., Moskvin, O.V., Toh, H., Wang, B., Zhang, J., Swanson, S., Guo, L.W., Thomson, J.A., and Slukvin, I.I. (2017). Specification and diversification of pericytes and smooth muscle cells from mesenchymoangioblasts. Cell Rep. *19*, 1902–1916.

Kurokawa, Y.K., Yin, R.T., Shang, M.R., Shirure, V.S., Moya, M.L., and George, S.C. (2017). Human induced pluripotent stem cell-derived endothelial cells for three-dimensional microphysiological systems. Tissue Eng. C Methods *23*, 474–484.

Kusuma, S., Shen, Y.-I., Hanjaya-Putra, D., Mali, P., Cheng, L., and Gerecht, S. (2013). Self-organized vascular networks from human pluripotent stem cells in a synthetic matrix. Proc. Natl. Acad. Sci. *110*, 12601–12606.

LeBleu, V.S., and Neilson, E.G. (2020). Origin and functional heterogeneity of fibroblasts. FASEB J. *34*, 3519–3536.

Lebrin, F., Goumans, M.-J., Jonker, L., Carvalho, R.L.C., Valdimarsdottir, G., Thorikay, M., Mummery, C., Arthur, H.M., and Dijke, P.ten (2004). Endoglin promotes endothelial cell proliferation and TGF-β/ALK1 signal transduction. EMBO J. *23*, 4018–4028.

Lee, A., Hudson, A.R., Shiwarski, D.J., Tashman, J.W., Hinton, T.J., Yerneni, S., Bliley, J.M., Campbell, P.G., and Feinberg, A.W. (2019). 3D bioprinting of collagen to rebuild components of the human heart. Science *365*, 482–487.

Lee-Montiel, F.T., Laemmle, A., Dumont, L., Lee, C.S., Huebsch, N., Charwat, V., Okochi, H., Hancock, M.J., Siemons, B., Boggess, S.C., et al. (2020). Integrated hiPSC-based liver and heart microphysiological systems predict unsafe drug-drug interaction. BioRxiv https://doi.org/10.1101/2020.05.24.112771.

Levato, R., Jungst, T., Scheuring, R.G., Blunk, T., Groll, J., and Malda, J. (2020). From shape to function: the next step in bioprinting. Adv. Mater. *32*, 1906423.

Lin, N.Y.C., Homan, K.A., Robinson, S.S., Kolesky, D.B., Duarte, N., Moisan, A., and Lewis, J.A. (2019). Renal reabsorption in 3D vascularized proximal tubule models. Proc. Natl. Acad. Sci. U S A *116*, 5399–5404.

Lin, Y., Jiang, W., Ng, J., Jina, A., and Wang, R.A. (2014). Endothelial Ephrin-B2 is essential for arterial vasodilation in mice. Microcirculation *21*, 578–586.

Linville, R.M., DeStefano, J.G., Sklar, M.B., Chu, C., Walczak, P., and Searson, P.C. (2020). Modeling hyperosmotic blood–brain barrier opening within human tissue-engineered in vitro brain microvessels. J. Cereb. Blood Flow Metab. *40*, 1517–1532.

Liu, C., Oikonomopoulos, A., Sayed, N., and Wu, J.C. (2018). Modeling human diseases with induced pluripotent stem cells: from 2D to 3D and beyond. Development *145*, dev156166.

Malek, A.M. (1999). Hemodynamic shear stress and its role in atherosclerosis. JAMA *282*, 2035.

Maoz, B.M., Herland, A., FitzGerald, E.A., Grevesse, T., Vidoudez, C., Pacheco, A.R., Sheehy, S.P., Park, T.-E., Dauth, S., Mannix, R., et al. (2018). A linked organ-on-chip model of the human neurovascular unit reveals the metabolic coupling of endothelial and neuronal cells. Nat. Biotechnol. *36*, 865–874.

Martin, T.A., Harding, K.G., and Jiang, W.G. (1999). Regulation of angiogenesis and endothelial cell motility by matrix-bound fibroblasts. Angiogenesis *3*, 69–76.

Mathur, A., Loskill, P., Hong, S., Lee, J., Marcus, S.G., Dumont, L., Conklin, B.R., Willenbring, H., Lee, L.P., and Healy, K.E. (2013). Human induced pluripotent stem cell-based microphysiological tissue models of myocardium and liver for drug development. Stem Cell Res. Ther. *4*, S14.

Mercurio, A., Sharples, L., Corbo, F., Franchini, C., Vacca, A., Catalano, A., Carocci, A., Kamm, R.D., Pavesi, A., and Adriani, G. (2019). Phthalimide derivative shows anti-angiogenic activity in a 3D microfluidic model and No teratogenicity in zebrafish embryos. Front. Pharmacol. *10*, 349.

Miller, J.S., Stevens, K.R., Yang, M.T., Baker, B.M., Nguyen, D.-H.T., Cohen, D.M., Toro, E., Chen, A.a, Galie, P.a, Yu, X., et al. (2012). Rapid casting of patterned vascular networks for perfusable engineered three-dimensional tissues. Nat. Mater. *11*, 768–774.

Morad, G., Carman, C.V., Hagedorn, E.J., Perlin, J.R., Zon, L.I., Mustafaoglu, N., Park, T.-E., Ingber, D.E., Daisy, C.C., and Moses, M.A. (2019). Tumor-derived extracellular vesicles breach the intact blood–brain barrier via transcytosis. ACS Nano *13*, 13853–13865.

Muller, W.A. (2013). Getting leukocytes to the site of inflammation. Vet. Pathol. *50*, 7–22.

Musah, S., Mammoto, A., Ferrante, T.C., Jeanty, S.S.F., Hirano-Kobayashi, M., Mammoto, T., Roberts, K., Chung, S., Novak, R., Ingram, M., et al. (2017). Mature induced-pluripotent-stem-cell-derived human podocytes reconstitute kidney glomerular-capillary-wall function on a chip. Nat. Biomed. Eng. *1*, 1–12.

Natividad-Diaz, S.L., Browne, S., Jha, A.K., Ma, Z., Hossainy, S., Kurokawa, Y.K., George, S.C., and Healy, K.E. (2019). A combined hiPSC-derived endothelial cell and in vitro microfluidic platform for assessing biomaterial-based angiogenesis. Biomaterials *194*, 73–83.

Naujok, O., Diekmann, U., and Lenzen, S. (2014). The generation of definitive endoderm from human embryonic stem cells is initially independent from Activin A but requires canonical wnt-signaling. Stem Cell Rev. Rep. *10*, 480–493.

Neal, E.H., Marinelli, N.A., Shi, Y., McClatchey, P.M., Balotin, K.M., Gullett, D.R., Hagerla, K.A., Bowman, A.B., Ess, K.C., Wikswo, J.P., et al. (2019). A simplified, fully defined differentiation scheme for producing blood-brain barrier endothelial cells from human iPSCs. Stem Cell Rep. *12*, 1380–1388.

Newman, A.C., Nakatsu, M.N., Chou, W., Gershon, P.D., and Hughes, C.C.W. (2011). The requirement for fibroblasts in angiogenesis: fibroblast-derived matrix proteins are essential for endothelial cell lumen formation. MBoC *22*, 3791–3800.

Newman, A.C., Chou, W., Welch-Reardon, K.M., Fong, A.H., Popson, S.A., Phan, D.T., Sandoval, D.R., Nguyen, D.P., Gershon, P.D., and Hughes, C.C.W. (2013). Analysis of stromal cell secretomes reveals a critical role for stromal cell–derived hepatocyte growth factor and fibronectin in angiogenesis. Arterioscler. Thromb. Vasc. Biol. *33*, 513–522.

Nguyen, D.-H.T., Stapleton, S.C., Yang, M.T., Cha, S.S., Choi, C.K., Galie, P.A., and Chen, C.S. (2013). Biomimetic model to reconstitute angiogenic sprouting morphogenesis in vitro. Proc. Natl. Acad. Sci. *110*, 6712–6717.

Nguyen, D.-H.T., Lee, E., Alimperti, S., Norgard, R.J., Wong, A., Lee, J.J.-K., Eyckmans, J., Stanger, B.Z., and Chen, C.S. (2019). A biomimetic pancreatic cancer on-chip reveals endothelial ablation via ALK7 signaling. Sci. Adv. *5*, eaav6789.

Niklason, L., and Dai, G. (2018). Arterial venous differentiation for vascular bioengineering. Annu. Rev. Biomed. Eng. *20*, 431–447.

Nikolova, G., Jabs, N., Konstantinova, I., Domogatskaya, A., Tryggvason, K., Sorokin, L., Fässler, R., Gu, G., Gerber, H.-P., Ferrara, N., et al. (2006). The vascular basement membrane: a niche for insulin gene expression and β cell proliferation. Dev. Cell *10*, 397–405.

Noor, N., Shapira, A., Edri, R., Gal, I., Wertheim, L., and Dvir, T. (2019). 3D printing of personalized thick and perfusable cardiac patches and hearts. Adv. Sci. *6*, 1900344.

Novak, R., Ingram, M., Marquez, S., Das, D., Delahanty, A., Herland, A., Maoz, B.M., Jeanty, S.S.F., Somayaji, M.R., Burt, M., et al. (2020). Robotic fluidic coupling and interrogation of multiple vascularized organ chips. Nat. Biomed. Eng. *4*, 407–420.

Nowak-Sliwinska, P., Alitalo, K., Allen, E., Anisimov, A., Aplin, A.C., Auerbach, R., Augustin, H.G., Bates, D.O., van Beijnum, J.R., Bender, R.H.F., et al. (2018). Consensus guidelines for the use and interpretation of angiogenesis assays. Angiogenesis *21*, 425–532.

Orlova, V.V., Van Den Hil, F.E., Petrus-Reurer, S., Drabsch, Y., Ten Dijke, P., and Mummery, C.L. (2014). Generation, expansion and functional analysis of endothelial cells and pericytes derived from human pluripotent stem cells. Nat. Protoc. *9*, 1514–1531.

Orlova Valeria, V., Yvette, D., Christian, F., Petrus-Reurer, S., van den Hil Francijna, E., Suchitra, M., Peter ten, D., and Mummery Christine, L. (2014). Functionality of endothelial cells and pericytes from human pluripotent stem cells demonstrated in cultured vascular plexus and zebrafish xenografts. Arterioscler. Thromb. Vasc. Biol. *34*, 177–186.

Park, T.-E., Mustafaoglu, N., Herland, A., Hasselkus, R., Mannix, R., FitzGerald, E.A., Prantil-Baun, R., Watters, A., Henry, O., Benz, M., et al. (2019). Hypoxia-enhanced blood-brain barrier chip recapitulates human barrier function and shuttling of drugs and antibodies. Nat. Commun. *10*, 2621.

Patsch, C., Challet-Meylan, L., Thoma, E.C., Urich, E., Heckel, T., O'Sullivan, J.F., Grainger, S.J., Kapp, F.G., Sun, L., Christensen, K., et al. (2015). Generation of vascular endothelial and smooth muscle cells from human pluripotent stem cells. Nat. Cell Biol. *17*, 994–1003.

Pavesi, A., Adriani, G., Rasponi, M., Zervantonakis, I.K., Fiore, G.B., and Kamm, R.D. (2015). Controlled electromechanical cell stimulation on-a-chip. Sci. Rep. *5*, 11800.

Perlingeiro, R.C.R. (2007). Endoglin is required for hemangioblast and early hematopoietic development. Development *134*, 3041–3048.

Phan, D.T.T., Wang, X., Craver, B.M., Sobrino, A., Zhao, D., Chen, J.C., Lee, L.Y.N., George, S.C., Lee, A.P., and Hughes, C.C.W. (2017). A vascularized and perfused organ-on-a-chip platform for large-scale drug screening applications. Lab Chip *17*, 511–520.

Prado-Lopez, S., Conesa, A., ArmiÃ±Ã¡n, A., MartÃ-nez-Losa, M., Escobedo-Lucea, C., Gandia, C., Tarazona, S., Melguizo, D., Blesa, D., Montaner, D., et al. (2009). Hypoxia promotes efficient differentiation of human embryonic stem cells to functional endothelium. Stem Cells *28*, 407–418.

Qiu, Y., Ahn, B., Sakurai, Y., Hansen, C.E., Tran, R., Mimche, P.N., Mannino, R.G., Ciciliano, J.C., Lamb, T.J., Joiner, C.H., et al. (2018). Microvasculature-on-a-chip for the long-term study of endothelial barrier dysfunction and microvascular obstruction in disease. Nat. Biomed. Eng. *2*, 453–463.

Ramasamy, S.K., Kusumbe, A.P., and Adams, R.H. (2015). Regulation of tissue morphogenesis by endothelial cell-derived signals. Trends Cell Biol. *25*, 148–157.

Reese, W.M., Burch, P., Korpusik, A.B., Liu, S.E., Loskill, P., Messersmith, P.B., and Healy, K.E. (2020). Facile macrocyclic polyphenol barrier coatings for PDMS microfluidic devices. Adv. Funct. Mater. *30*, 2001274.

Resnick, N., Collins, T., Atkinson, W., Bonthront, D.T., Dewey, C.F., and Gimbrone, M.A. (1993). Platelet-derived growth factor B chain promoter contains a cis-acting fluid shear-stress-responsive element. Proc Natl Acad Sci U S A *90*, 4591–4595.

Romero-López, M., Trinh, A.L., Sobrino, A., Hatch, M.M.S., Keating, M.T., Fimbres, C., Lewis, D.E., Gershon, P.D., Botvinick, E.L., Digman, M., et al. (2017). Recapitulating the human tumor microenvironment: colon tumor-derived extracellular matrix promotes angiogenesis and tumor cell growth. Biomaterials *116*, 118–129.

Rosa, S., Praça, C., Pitrez, P.R., Gouveia, P.J., Aranguren, X.L., Ricotti, L., and Ferreira, L.S. (2019). Functional characterization of iPSC-derived arterial- and venous-like endothelial cells. Sci. Rep. *9*, 3826.

Salminen, A.T., Zhang, J., Madejski, G.R., Khire, T.S., Waugh, R.E., McGrath, J.L., and Gaborski, T.R. (2019). Ultrathin dual-scale nano- and microporous membranes for vascular transmigration models. Small *15*, 1804111.

Sandoo, A., Veldhuijzen van Zanten, J.J.C.S., Metsios, G.S., Carroll, D., and Kitas, G.D. (2010). The endothelium and its role in regulating vascular tone. TOCMJ *4*, 302–312.

Satchell, S.C., and Braet, F. (2009). Glomerular endothelial cell fenestrations: an integral component of the glomerular filtration barrier. Am. J. Physiol. Renal. Physiol. *296*, F947–F956.

Sewell-Loftin, M.K., Bayer, S.V.H., Crist, E., Hughes, T., Joison, S.M., Longmore, G.D., and George, S.C. (2017). Cancer-associated fibroblasts support vascular growth through mechanical force. Sci. Rep. *7*, 12574.

Sewell-Loftin, M.K., Katz, J.B., George, S.C., and Longmore, G.D. (2020). Micro-strains in the extracellular matrix induce angiogenesis. Lab Chip *20*, 2776–2787.

Shamis, Y., Silva, E.A., Hewitt, K.J., Brudno, Y., Levenberg, S., Mooney, D.J., and Garlick, J.A. (2013). Fibroblasts derived from human pluripotent stem cells activate angiogenic responses in vitro and in vivo. PLoS One *8*, e83755.

Shin, Y., Jeon, J.S., Han, S., Jung, G.-S., Shin, S., Lee, S.-H., Sudo, R., Kamm, R.D., and Chung, S. (2011). In vitro 3D collective sprouting angiogenesis under orchestrated ANG-1 and VEGF gradients. Lab Chip *11*, 2175.

Shin, Y., Choi, S.H., Kim, E., Bylykbashi, E., Kim, J.A., Chung, S., Kim, D.Y., Kamm, R.D., and Tanzi, R.E. (2019). Blood–brain barrier dysfunction in a 3D in vitro model of Alzheimer's disease. Adv. Sci. *6*, 1900962.

Skylar-Scott, M.A., Uzel, S.G.M., Nam, L.L., Ahrens, J.H., Truby, R.L., Damaraju, S., and Lewis, J.A. (2019). Biomanufacturing of organ-specific tissues with high cellular density and embedded vascular channels. Sci. Adv. *5*, eaaw2459.

Sobrino, A., Phan, D.T.T., Datta, R., Wang, X., Hachey, S.J., Romero-López, M., Gratton, E., Lee, A.P., George, S.C., and Hughes, C.C.W. (2016). 3D microtumors in vitro supported by perfused vascular networks. Sci. Rep. *6*, 31589.

Song, K.H., Highley, C.B., Rouff, A., and Burdick, J.A. (2018). Complex 3D-printed microchannels within cell-degradable hydrogels. Adv. Funct. Mater. *28*, 1801331.

Stebbins, M.J., Gastfriend, B.D., Canfield, S.G., Lee, M.-S., Richards, D., Faubion, M.G., Li, W.-J., Daneman, R., Palecek, S.P., and Shusta, E.V. (2019). Human pluripotent stem cell–derived brain pericyte–like cells induce blood-brain barrier properties. Sci. Adv. *5*, eaau7375.

Teuwen, L.-A., Geldhof, V., Pasut, A., and Carmeliet, P. (2020). COVID-19: the vasculature unleashed. Nat. Rev. Immunol. *20*, 389–391.

Thomas, M., and Augustin, H.G. (2009). The role of the angiopoietins in vascular morphogenesis. Angiogenesis *12*, 125.

Tiemeier, G.L., Wang, G., Dumas, S.J., Sol, W.M.P.J., Avramut, M.C., Karakach, T., Orlova, V.V., van den Berg, C.W., Mummery, C.L., Carmeliet, P., et al. (2019). Closing the mitochondrial permeability transition pore in hiPSC-derived endothelial cells induces glycocalyx formation and functional maturation. Stem Cell Rep. *13*, 803–816.

Trappmann, B., Baker, B.M., Polacheck, W.J., Choi, C.K., Burdick, J.A., and Chen, C.S. (2017). Matrix degradability controls multicellularity of 3D cell migration. Nat. Commun. *8*, 371.

Varga, Z., Flammer, A.J., Steiger, P., Haberecker, M., Andermatt, R., Zinkernagel, A.S., Mehra, M.R., Schuepbach, R.A., Ruschitzka, F., and Moch, H. (2020). Endothelial cell infection and endotheliitis in COVID-19. Lancet *395*, 1417–1418.

Vatine, G.D., Barrile, R., Workman, M.J., Sances, S., Barriga, B.K., Rahnama, M., Barthakur, S., Kasendra, M., Lucchesi, C., Kerns, J., et al. (2019). Human iPSC-derived blood-brain barrier chips enable disease modeling and personalized medicine applications. Cell Stem Cell *24*, 995–1005.e6.

Vickerman, V., Blundo, J., Chung, S., and Kamm, R. (2008). Design, fabrication and implementation of a novel multi-parameter control microfluidic platform for three-dimensional cell culture and real-time imaging. Lab Chip *8*, 1468.

Walshe, T.E., Saint-Geniez, M., Maharaj, A.S.R., Sekiyama, E., Maldonado, A.E., and D'Amore, P.A. (2009). TGF-beta is required for vascular barrier function, endothelial survival and homeostasis of the adult microvasculature. PLoS One *4*, e5149.

Wang, N., Zhang, R., Wang, S.-J., Zhang, C.-L., Mao, L.-B., Zhuang, C.-Y., Tang, Y.-Y., Luo, X.-G., Zhou, H., and Zhang, T.-C. (2013). Vascular endothelial growth factor stimulates endothelial differentiation from mesenchymal stem cells via Rho/myocardin-related transcription factor-A signaling pathway. Int. J. Biochem. Cell Biol. *45*, 1447–1456.

Wanjare, M., Kusuma, S., and Gerecht, S. (2013). Perivascular cells in blood vessel regeneration. Biotechnol. J. *8*, 434–447.

Wanjare, M., Kusuma, S., and Gerecht, S. (2014). Defining differences among perivascular cells derived from human pluripotent stem cells. Stem Cell Rep. *2*, 561–575.

Ware, B.R., Durham, M.J., Monckton, C.P., and Khetani, S.R. (2018). A cell culture platform to maintain long-term phenotype of primary human hepatocytes and endothelial cells. Cell Mol. Gastroenterol. Hepatol. *5*, 187–207.

Yamane, A., Yamaguchi, S., and Seetharam, L. (1994). A new communication system between hepatocytes and sinusoidal endothelial cells in liver through vascular endothelial growth factor and Flt tyrosine kinase receptor family (Flt-1 and KDR/Flk-1). Oncogene *9*, 2683-2690.

Yeste, J., García-Ramírez, M., Illa, X., Guimerà, A., Hernández, C., Simó, R., and Villa, R. (2017). A compartmentalized microfluidic chip with crisscross microgrooves and electrophysiological electrodes for modeling the blood-retinal barrier. Lab Chip *18*, 95–105.

Yu, J., Cilfone, N.A., Large, E.M., Sarkar, U., Wishnok, J.S., Tannenbaum, S.R., Hughes, D.J., Lauffenburger, D.A., Griffith, L.G., Stokes, C.L., et al. (2015). Quantitative systems pharmacology approaches applied to microphysiological systems (MPS): data interpretation and multi-MPS integration. CPT Pharmacometrics Syst. Pharmacol. *4*, 585–594.

Zanone, M.M., Favaro, E., Ferioli, E., Huang, G.C., Klein, N.J., Perin, P.C., Peakman, M., Conaldi, P.G., and Camussi, G. (2007). Human pancreatic islet endothelial cells express coxsackievirus and adenovirus receptor and are activated by coxsackie B virus infection. FASEB J. *21*, 3308–3317.

Zervantonakis, I.K., Hughes-Alford, S.K., Charest, J.L., Condeelis, J.S., Gertler, F.B., and Kamm, R.D. (2012). Three-dimensional microfluidic model for tumor cell intravasation and endothelial barrier function. Proc. Natl. Acad. Sci. *109*, 13515–13520.

Zhang, B., Montgomery, M., Chamberlain, M.D., Ogawa, S., Korolj, A., Pahnke, A., Wells, L.A., Masse, S., Kim, J., Reis, L., et al. (2016a). Biodegradable scaffold with built-in vasculature for organ-on-a-chip engineering and direct surgical anastomosis. Nat. Mater. *15*, 669–678.

Zhang, H., Tian, L., Shen, M., Tu, C., Wu, H., Gu, M., Paik, D.T., and Wu, J.C. (2019). Generation of quiescent cardiac fibroblasts from human induced pluripotent stem cells for in vitro modeling of cardiac fibrosis. Circ. Res. *125*, 552–566.

Zhang, J., Chu, L.-F., Hou, Z., Schwartz, M.P., Hacker, T., Vickerman, V., Swanson, S., Leng, N., Nguyen, B.K., Elwell, A., et al. (2017). Functional characterization of human pluripotent stem cell-derived arterial endothelial cells. Proc. Natl. Acad. Sci. U S A *114*, E6072–E6078.

Zhang, Y.S., Arneri, A., Bersini, S., Shin, S.-R., Zhu, K., Goli-Malekabadi, Z., Aleman, J., Colosi, C., Busignani, F., Dell'Erba, V., et al. (2016b). Bioprinting 3D microfibrous scaffolds for engineering endothelialized myocardium and heart-on-a-chip. Biomaterials *110*, 45–59.

Zhao, Z., Nelson, A.R., Betsholtz, C., and Zlokovic, B.V. (2015). Establishment and dysfunction of the blood-brain barrier. Cell *163*, 1064–1078.

Zheng, Y., Chen, J., Craven, M., Choi, N.W., Totorica, S., Diaz-Santana, A., Kermani, P., Hempstead, B., Fischbach-Teschl, C., Lopez, J.A., et al. (2012). In vitro microvessels for the study of angiogenesis and thrombosis. Proc. Natl. Acad. Sci. *109*, 9342–9347.